Nat. Hazards Earth Syst. Sci., 13, 1873–1887, 2013
www.nat-hazards-earth-syst-sci.net/13/1873/2013/
doi:10.5194/nhess-13-1873-2013

Natural Hazards and Earth System Sciences
Open Access

Non-interferometric GB-SAR measurement: application to the Vallcebre landslide (eastern Pyrenees, Spain)

O. Monserrat[1], J. Moya[2], G. Luzi[1], M. Crosetto[1], J. A. Gili[2], and J. Corominas[2]

[1]Institute of Geomatics, Castelldefels, Barcelona, Spain
[2]Dept. of Geotechnical Engineering and Geosciences, Technical University of Catalonia-BarcelonaTech, Barcelona, Spain

Correspondence to: O. Monserrat (oriol.monserrat@ideg.es)

Received: 10 December 2012 – Published in Nat. Hazards Earth Syst. Sci. Discuss.: –
Revised: 5 April 2013 – Accepted: 23 May 2013 – Published: 29 July 2013

Abstract. In the last decade, ground-based interferometry has proven to be a powerful technique for continuous deformation monitoring of landslides, glaciers, volcanoes, or man-made structures, among others. However, several limitations need to be addressed in order to improve the performances of the technique, especially for long-term monitoring. These limitations include the reduction of measurable points with an increase in the period of observation, the ambiguous nature of the phase measurements, and the influence of the atmospheric phase component. In this paper, a new procedure to process the amplitude component of ground-based synthetic aperture radar (GB-SAR) data acquired in discontinuous mode is compared and validated. The use of geometric features of the amplitude images combined with a matching technique will allow the estimation of the displacements over specific targets. Experimental results obtained during 19 months, in eight different campaigns carried out in the active landslide of Vallcebre (eastern Pyrenees, Spain), were analysed. During the observed period, from February 2010 to September 2011, displacements up to 80 cm were measured. The comparison with other surveying technique shows that the precision of the method is below 1 cm.

1 Introduction

In the last few years the ground-based synthetic aperture radar (GB-SAR) interferometry has demonstrated to be a useful technique for deformation measurement in a wide range of applications such as landslides (Pieraccini et al., 2002; Leva et al., 2003; Tarchi et al., 2003; Antonello et al., 2004; Del Ventisette et al., 2011; Herrera et al., 2009), dams (Tarchi et al., 1999 and Alba et al., 2008), glaciers (Luzi et al., 2007; Strozzi et al., 2011), and volcano slopes (e.g. Casagli et al., 2009, 2010; Antonello et al., 2003 and Rödelsperger et al., 2010). For a general review of the GB-SAR interferometry see Luzi (2010).

The GB-SAR interferometric technique requires two fundamental components: a coherent GB-SAR sensor, which measures both the phase and the amplitude of the backscattered radar signal, and repeated SAR acquisitions (at least two) of the same scene over time. The displacements occurred between two SAR acquisitions in the observed scene can be derived by computing and analysing the interferometric phase calculated from the acquired images. The main advantage of this technique is its high sensitivity to small displacements, which can be measured with a precision that is a fraction of the used SAR wavelength. Considering that most of the available GB-SAR systems operate in the 1.7–5.8 cm wavelength region (corresponding to Ku- and C band, respectively), a millimetric or even sub-millimetric displacement precision can be achieved. However, although GB-SAR interferometry has been successfully used in a wide range of applications, it suffers some limitations that can be critical in some cases. The first limitation is that not all the measured points can be exploited by SAR interferometry: the capability of exploiting the phase for deformation measurement is limited by the noise of the point. The level of noise of a point is usually estimated using different statistical parameters such as the amplitude dispersion over time (DA) or the spatial behaviour of the phase (coherence). The loss of coherence that SAR data may experience over time can be particularly severe over vegetated and forested areas, and over scenes that change continuously, modifying their radar responses. This

aspect critically affects the GB-SAR discontinuous monitoring of very slow deformation phenomena, where the lapse of time between two image acquisitions ranges from some weeks to several months or years. A second critical limitation is the so-called aliasing effect. GB-SAR interferometry exploits phase differences between measurements of the same area at different times. Although the technique provides millimetre sensitivity, because it measures displacements within a portion of the wavelength, it is not capable to measure unambiguously displacements larger than a quarter of the wavelength. From the operational point of view, the risk of deriving ambiguous displacement estimates represents a very severe limitation of the technique. A third limitation is related to the atmospheric component of the interferometric phase, caused by relative changes of humidity, temperature and pressure of the air at the time of acquisition of the SAR images (see Noferini et al., 2005). The atmospheric effect may degrade the quality of the displacement estimation. In the worst cases, when strong atmospheric components are associated with spatially sparse coherent targets, it may even affect phase unwrapping (see Monserrat et al., 2012). Finally, GB-SAR interferometry can only retrieve the component of the actual displacement corresponding to the line-of-sight (LOS) direction of the radar.

GB-SAR interferometry can be applied in two data acquisition modes (Monserrat et al., 2012): the continuous mode, which consists in leaving the sensor installed without interrupting the acquisition; and the discontinuous mode, which is based on removing and re-placing the system in each campaign separated, typically, by weeks to months. The first one is appropriate for monitoring either landslides with moderate velocity or landslide crisis, in which movement accelerates significantly. The latter is more appropriate to monitor slow or very slow displacement rates (see Cruden and Varnes, 1996). Although the above-mentioned limitations affect both approaches, it is in the discontinuous mode where the loss of coherence and the aliasing errors can particularly compromise the applicability of the technique.

To overcome these drawbacks, a new approach using the amplitude component of GB-SAR observations acquired in discontinuous mode, described in Crosetto et al. (2013a), has been tested and applied in the Vallcebre landslide. This approach provides remarkable improvements in the above-mentioned limitations with respect to the results achievable with the interferometric approach. This landslide has been selected to test this novel procedure because it is a slow one (about $25\,\mathrm{cm\,yr^{-1}}$), the interferometric approach does not present the best performances, and its behaviour is well known because it has been continuously monitored during the last years (Corominas et al., 2000).

The paper is structured into five main sections: after the introduction, in Sect. 2 the main points of the used procedure are briefly described; Sect. 3 describes the obtained results and discusses validation results obtained from its comparison with total station and wire extensometer measurements; then in Sect. 4 the results are analysed from the geological point of view and finally some conclusions are drawn.

2 Non-interferometric GB-SAR

The non-interferometric GB-SAR procedure used in this work takes full advantage of the GB-SAR imagery by jointly using an image-matching technique applied to the amplitude data of the GB-SAR images and specific targets, which allows optimizing the performances of the image-matching technique. These targets can be either artificial corner reflectors (CRs) or natural targets already available to sample the phenomenon of interest. Herein we apply the term CR to both natural and artificial reflectors that are "good" from the point of view of the proposed procedure.

The main concept of the procedure is illustrated in Fig. 1; two images of the same area collected at different times (master and slave) are used. Then by using a matching algorithm, the same point on both images is detected and the displacement vector (S_x, S_y) that connects P to P' is estimated at sub-pixel level. Figure 2 shows the sequence of the entire procedure. A detailed description of the procedure, which is here briefly described, can be found in Crosetto et al. (2013):

- Data acquisition: data acquisition is carried out through a series of N in situ campaigns. In each campaign the GB-SAR instrument is installed, a set of M CRs is deployed in both stable and unstable areas of the area of interest (AoI), and K complex SAR images are acquired.

- Data pre-processing: this step is performed for every set of images acquired in a campaign. It consist of checking the quality of each acquired complex SAR image in order to detect and eventually discard anomalous images corrupted by fortuitous noise. A temporal filtering, whose goal is image enhancement by strongly reducing the so-called speckle effect, is then performed on the sub-set of $Q \leq K$ quality-assured images.

- Global matching and estimation of the GB-SAR repositioning effects: these steps are performed on each analysed pair (i, j) of campaigns. CRs located in stable areas are used to estimate and correct the error in the repositioning of the GB-SAR sensor between different campaigns.

- Estimation of the pairs of displacements: this step is performed on each analysed pair (i, j) of campaigns by subtracting the GB-SAR-repositioning error, estimated on the previous step, to the selected CRs distributed along the scene (both stable and unstable areas). It results in $R < M$ pairs of displacement shifts, where the displacements are relative to the whole set of stable areas mentioned above.

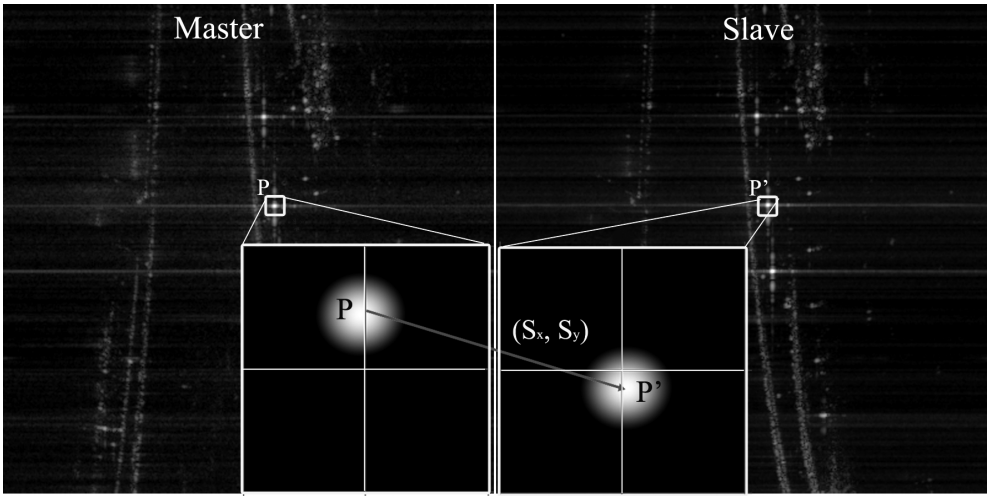

Fig. 1. Two GB-SAR amplitude images, master and slave, collected over the same place. The same point is identified in both images, P and P', and then the displacement vector (S_x, S_y) is estimated at sub-pixel level as shown in the small frames.

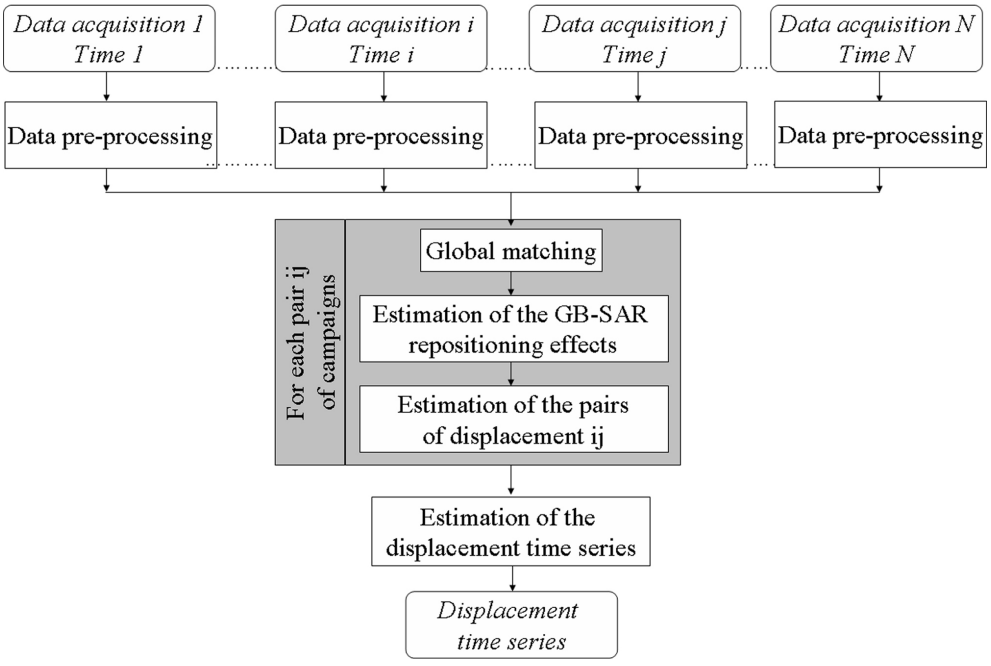

Fig. 2. Diagram of the GB-SAR non-interferometric procedure.

– Estimation of the displacement time series: this step is applied once for all campaigns in order to obtain the main product of the procedure – the estimated displacement time series. As described in Crosetto et al. (2013), the displacement time series are estimated through an iterative least-squares (LS) estimation procedure.

It is worth noting that the use of the amplitude component of the SAR images allows, under certain conditions, overcoming the limitations of the interferometric approach discussed above. In this regard, the main advantages of the non-interferometric approach are as follows: (i) it provides non-ambiguous displacement estimates, (ii) the atmospheric effects are negligible compared to the precision of the method, and (iii) it yields 2-D displacement measurements in range and cross-range directions. In addition, by employing CRs, precise and reliable displacement estimates can be achieved. It is important to underline that displacements over single targets are estimated with the non-interferometric procedure, while SAR amplitude matching is usually employed for co-registration purposes, where hundreds of points are used to estimate a limited set of parameters (usually less than 10 for

the entire image). In this context, where we need to rely on the two displacements (shifts) per each measured target, CRs are fundamental.

The quality of the measurements is evaluated by the peak-to-background-ratio (PBR) parameter. Crosetto et al. (2013a) demonstrate that PBR greater than 30 dB is required to obtain a precision of 1/50 pixels on the shift estimation. Considering the GB-SAR imaging parameters used in this work, 1/50 pixels of precision means a displacement in deformation estimate of 1 cm.

3 The Vallcebre landslide monitoring

The Vallcebre landslide is an active landslide that is very sensitive to changes in the water table levels. The main interest of this landslide lies in its relatively simple geometry and geology, and its low velocity. These characteristics allow testing monitoring sensors and techniques more easily and carrying out mechanical and hydrological modelling to reproduce the slope behaviour. The Vallcebre landslide, which can be considered to be a real-scale laboratory, has been used to assess the performance of different monitoring techniques such as precise differential GPS (Gili et al., 2000), borehole wire extensometers (Corominas et al., 2000), and satellite radar interferometry (Crosetto et al., 2013b) in the last two decades. GB-SAR is the technique applied most recently to monitor the displacement of the landslide. The results of the monitoring activities carried out in the Vallcebre landslide are described in this section.

3.1 General description of the landslide and the monitoring network

The Vallcebre landslide is a large and active translational landslide located in the upper Llobregat river basin, in the eastern Pyrenees, 125 km north of Barcelona, Spain (Fig. 3). It develops in a gentle slope of about 10° on average. The landslide is 1200 m long and 600 m wide, involving an area of 0.8 km^2. The mobilized material consists of a set of shale, gypsum, siltstone, and claystone layers gliding over a thick limestone unit. This sedimentary sequence is of upper Cretaceous–lower Palaeocene age and is folded forming an open syncline whose axis is dipping nearly towards the down-slope direction. The landslide involves mainly silty-claystone layers and gypsum lenses (Corominas et al., 2000, 2005).

The slide is formed by three main units. Each unit has a gentle slope surface bounded in its head by a scarp a few tens of metres high. The lower unit is the most active one. Most of the evidence of superficial deformation is located at the boundaries of the slide units as distinct lateral shear surfaces and tension cracks. Other cracks are placed at the bottom of the head scarp of each slide unit. Within the landslide units, in contrast, the ground surface is only disturbed by minor scarps and by some cracking of the walls of the few farmhouses that are located in the landslide intermediate unit. These houses and a couple of roads that cross the landslide are the only elements at risk present in the slope.

The Vallcebre landslide was first monitored in 1987 using conventional surveying and photogrammetry. From 1996 to 1998, eight boreholes were equipped with conventional inclinometers and another six with wire extensometers and open pipe piezometers (Corominas et al., 2000, 2005). Since 1996, systematic recording of landslide displacements in wire extensometers is carried out every 20 min. Nowadays, three of the borehole wire extensometers are operational after 15 yr of recording. Horizontal displacements of up to 3.9 m were observed at some points (S2 borehole of Fig. 3) along these 15 yr, with an average velocity of 25 cm yr^{-1}.

Superficial displacements have also been measured using global positioning satellite systems (GPS, GNSS) since December 1995 in 30 control points, which include the borehole ends with wire extensometers (Gili et al., 2000). Precise differential GPS observations allowed obtaining a more distributed view of the landslide displacement and, at the same time, calibrating the displacements measured by wire extensometers during the early stages of the operation (Corominas et al., 2000). GPS campaigns were carried out bimonthly between 1995 and 1998, and there is one campaign per year currently.

Satellite differential interferometric SAR (DInSAR) techniques have been used in the Vallcebre landslide since 2006 with the aim of improving the number and distribution of the control points in the landslide and to calibrate the technique. DInSAR monitoring of the landslide has been carried out by analysing 15 Envisat images, covering the period December 2006 to December 2008. Seven artificial CRs were used in the analysis because the landslide is densely vegetated and natural reflectors are scarce; see Crosetto et al. (2013b). Moreover, between February 2010 and September 2011, 15 CRs distributed in and around the lower unit of the landslide were deployed to evaluate the performance of the non-interferometric GB-SAR approach. In this period, eight measurements campaigns were carried out using the IBIS-L Ku-band GB-SAR, constructed and marketed by IDS SpA (Fig. 4). Table 1 summarizes the main parameters of the radar system. It is important to note that the size of the pixel is not homogeneous, due to the radar processing (focusing algorithm), and along the cross-range direction it depends linearly on the range from the radar position (Fortuny-Guasch, 2009).

3.2 GB-SAR measurements: description and validation

Figure 5 shows a picture of the monitored area where the active part of the landslide is bounded by the black line. The grey dots represent the 11 CRs deployed in the unstable area, while the four white dots represent the reference CRs, which were assumed to be stable during the measured period. The

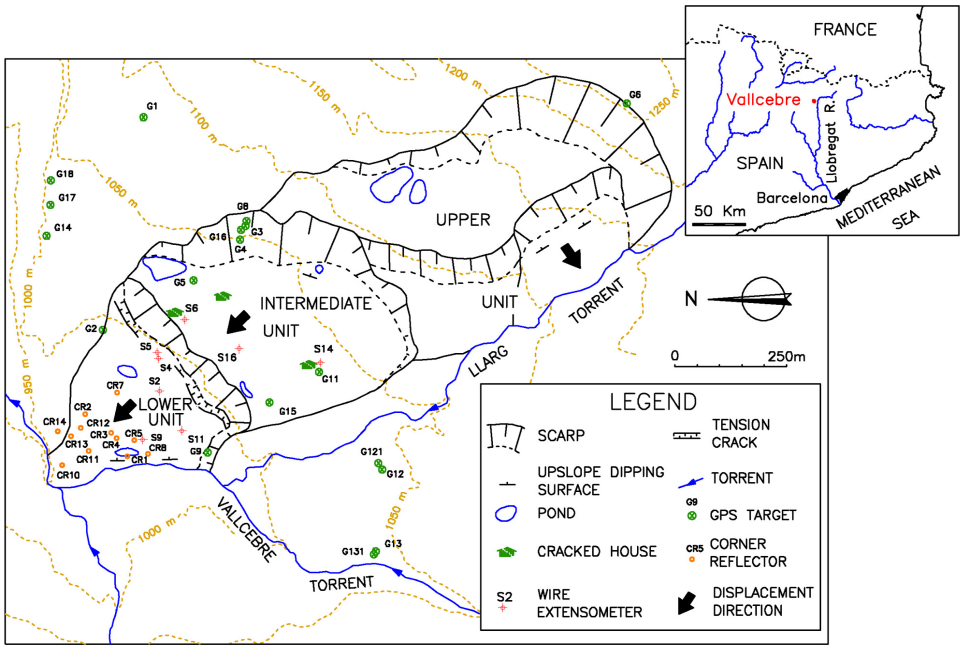

Fig. 3. Geomorphological sketch of the Vallcebre landslide (Corominas et al., 2005).

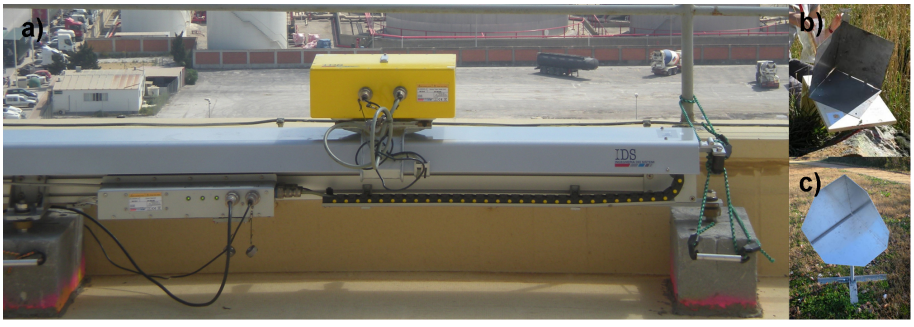

Fig. 4. (a) Picture of the GB-SAR system used in this work. The synthetic aperture is obtained through the movement of the radar sensor (yellow box) along the rail. **(b)**"First-generation CRs". **(c)**" New-generation CRs".

reference CRs, together with other natural reflectors, were used to estimate the repositioning effects.

In parallel to the GB-SAR measurements, five surveying campaigns were carried out to validate the results obtained with the GB-SAR. A total station was set up at the same position of the GB-SAR and the distances to the CRs were measured with the electronic distance meter (EDM). In order to assure the millimetre precision needed to validate the GB-SAR displacements and to ease the validation analysis, several control points distributed along the scenario were measured several times on each survey. This control points were used to assure correct repositioning, good atmospheric effects correction, and to evaluate the final accuracy of the measurements, which was estimated as 2.6 mm. It is important to note that the results concerning GB-SAR and total station are both in LOS and that it was not possible to reinstall the 15 CRs in all the campaigns due to changes in vegetation and water level rises in a portion of the monitored area.

Two different types of CRs were used along the monitored period. For the first four campaigns 30 cm sized trihedral CRs, herein called "first generation CRs", were used (Fig. 4b), which allowed a light repositioning by simply marking with paint the position of each CR on stones. However, the repositioning errors were of the same order of magnitude of the precision of the procedure limiting the analysis. In addition, due to the target–sensor distance, it was not possible to achieve the best performances in terms of deformation measurement precision with these CRs; that is, it was not possible to obtain the required 30 dB of PBR. The first section of Table 2, measurement 07/2010–09/2010, shows the results obtained using these reflectors and its comparison with EDM results. Despite the relatively low PBR, half

Fig. 5. Location of the GB-SAR CRs and the used extensometers on the Vallcebre test site. The white dots indicate the CRs located in stable areas, while the grey dots are the CRs deployed on the sliding area (black line bounded). Eastwards view from the GB-SAR base station.

Table 1. Main parameters of the GB-SAR system used in this work.

Parameter	Value
Operating frequency / wavelength	17 GHz (Ku band)/ 17.6 mm
Maximum operational distance	4000 m
Spatial resolution: range / cross range @ 1 km	0.5 m / 4.5 m
Minimum acquisition rate	5 min
Weight of the whole system	130 kg
Rail length	2 m
Power consumption	0.80 W

of the measurements have errors of about 1 cm or less, while the other half have errors above 2 cm. It is worth noting that these errors could be caused by both matching errors and errors of repositioning of the CRs.

In order to improve the performances of the method, a new set of CRs, the "new-generation CRs", was developed. These are composed of a square trihedral of 50 cm and a base (Fig. 4c). The bases of the CRs were fixed mechanically to the terrain (e.g. rocks, boulders) and remained in situ during the experiment, while the CR heads were removed and installed at each campaign. The "new-generation CRs" allowed improving the precision on the repositioning noticeably and obtaining higher PBR as shown in Table 2, measurement 11/2010–01/2011 and 01/2011–04/2011. In fact, the PBR ratio was greater than 30 dB for all CRs. In this case, the comparison with the EDM shows that all the measurements but one display errors around 1 cm. There is only one outlier (CR9, measurement 11/2010–01/2011, Table 2) probably caused by an error in the repositioning of the total station prism. Without considering CR9, the dispersion of the GB-SAR error is 0.7 cm. To conclude, it is worth noting that although Table 2 shows that CR17 moved around 2 cm in both measurements (1 order of magnitude smaller than other CRs), it has been considered stable because in most of campaigns it remained basically stable compared to the most active part of the landslide, and, taking into account that from the point of view of the global matching, its location has helped to improve the GB-SAR repositioning error correction.

Figure 6 shows an aerial photo of the observed area with the LOS displacement vectors estimated for the CRs during the period February 2010 to September 2010. Figure 7 shows the time series of the eight CRs which were repositioned in all the campaigns during the period February 2009 to September 2011. During this period, the maximum measured LOS displacement is 80.1 cm and corresponds to CR12. The

Table 2. GB-SAR results for three measurements on Vallcebre test site and their comparison with EDM results.

	CR	Target–sensor distance [m]	EDM-measured displ. [cm]	GB-SAR- measured displ. [cm]	GB-SAR error [cm]	PBR [dB]
Period: 07/2010–09/2010 (First-generation CRs)	CR03	532.0	−4.2	−7.0	2.83	27
	CR04	523.5	−4.3	−5.5	1.17	20
	CR05	546.0	−3.9	−6.3	2.35	21
	CR06	600.5	−3.9	−9.4	5.48	24
	CR07	619.5	−4.4	−5.5	1.07	21
	CR08	526.5	−3.5	−3.1	−0.38	20
	CR10	441.0	−2.2	−4.7	2.49	21
	CR12	530.5	−4.4	−4.7	0.29	27
	CR14	524.5	0.3	0.8	−0.48	14
Period: 11/2010–01/2011 (New-generation CRs)	CR01	507.0	−3.7	−4.9	1.26	34
	CR03	533.0	−4.2	−4.2	−0.03	33
	CR05	543.5	−4.1	−2.6	−1.49	31
	CR06	600.0	−3.9	−3.4	−0.51	33
	CR09	445.5	−4.7	−9.6	4.94	33
	CR10	440.5	−3.7	−3.4	−0.31	32
	CR11	482.0	−4.3	−4.9	0.66	35
	CR12	530.5	−5.0	−4.9	−0.04	33
	CR14	523.5	0.4	−0.3	0.67	34
	CR15	707.5	0.6	−0.3	0.87	33
	CR16	466.5	0.0	0.5	−0.47	34
	CR17	832.5	−2.3	−2.6	0.31	30
Period: 01/2011–04/2011 (New-generation CRs)	CR01	507.0	−9.8	−8.9	−0.88	34
	CR03	533.0	−10.6	−10.1	−0.57	34
	CR05	543.5	−10.6	−10.1	−0.57	34
	CR06	600.0	−9.0	−9.7	0.65	35
	CR09	445.5	−8.5	−8.9	0.36	34
	CR10	440.5	−8.0	−7.2	−0.86	34
	CR11	482.0	−9.9	−10.4	0.52	35
	CR12	530.5	−11.4	−11.2	−0.20	34
	CR14	523.5	0.7	0.9	−0.18	34
	CR15	707.5	0.8	0.1	0.70	36
	CR16	466.5	0.9	0.1	0.80	34
	CR17	832.5	−1.8	−1.1	−0.75	31

time series show that the movements are roughly linear in time, displaying a deceleration of the displacements between July 2010 and January 2011 followed by an increase of the activity. This behaviour is explained by a decrease of the water table during the period of deceleration of the displacement (see Corominas et al., 2005).

3.3 Comparison of GB-SAR data with wire extensometer measurements

In the previous section, the displacements estimated using the non-interferometric GB-SAR technique have been compared with those obtained with classical surveying (EDM) providing a validation of the LOS GB-SAR measurements. However, in terms of actual landslide displacement, the above validation does not provide a rigorous assessment because both techniques are measuring the CRs. To evaluate the consistency of the GB-SAR results in terms of landslide displacement, a comparison with the results coming from two wire extensometers located at different points of the landslide was carried out. In this case, the wire extensometers provided independent measurement of the total displacement with 1 mm of accuracy.

The comparison was carried out using the CRs 5 and 7 and the extensometers S11 and S2. These corner reflectors are not located in the same position as the extensometers, which would be the ideal case, but some tens of metres away. Wire extensometers were distributed in Vallcebre along two

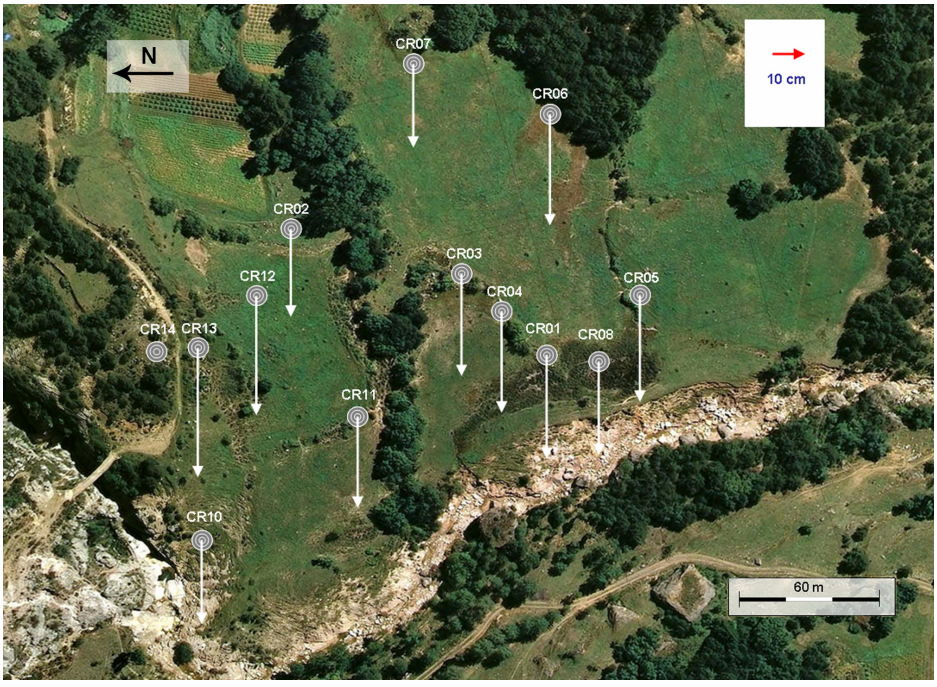

Fig. 6. Aerial photo of the measured area with the accumulated displacement vectors for those CRs with reliable results in the period February 2010 to September 2010. Note that only the magnitude is plotted. The maximum measured displacement in this period corresponds to CR13 with 39.8 cm. The aerial photo is courtesy of the Cartographic Institute of Catalonia.

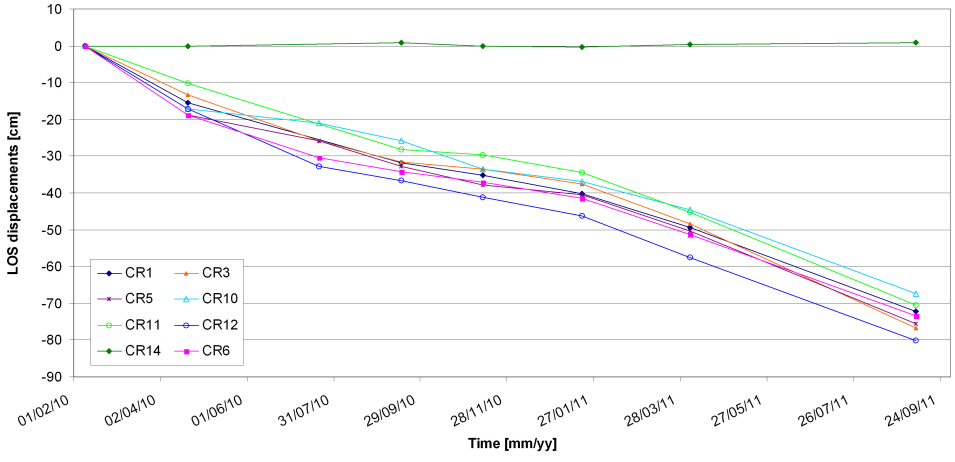

Fig. 7. Measured displacements between February 2010 and September 2011 at eight CRs (see location in Fig. 5). Only those CRs with a full record line are plotted.

cross sections, at points considered representative of the landslide behaviour, as the landslide morphology suggested, and most of them were installed within the forested area. However, CRs for GB-SAR measurement were placed at points with direct view from the radar base station, avoiding forested zones, and trying to cover areas of the landslide that were not being monitored by extensometers and GPS. A CR (CR5) was installed very close to the only extensometer that is placed at the foot of the landslide (S9), which is unforested (Fig. 3). Unfortunately, data from this extensometer revealed that it broke before the onset of the GB-SAR measurements, and therefore it could not be used directly in the validation. Despite this, the translational nature of the landslide allows the use of a wire extensometer located a few tens of metres away in the same slide unit, and with no scarps or cracks situated in between. instead. The distances between CR5 and S11, and CR7 and S2, are 96 and 85 m, respectively. At these distances, some minor relative displacements between the CR and the extensometers can be expected, as is analysed below.

Table 3. Comparison of GB-SAR LOS displacements (D_{LOS}) measured for CR5 and CR7 and total displacements measured by wire extensometers (D_W) for S11 and S2, respectively.

Date	D_{LOS}CR5 [cm]	D_WS11 [cm]	$D_{LOS} - D_W/D_W$[%] (CR5, S11)	D_SCR7 [cm]	D_WS2 [cm]	$D_{LOS} - D_W/D_W$ [%] (CR7, S2)
09/02/2010	0.0	0.0	–	0.0	0.0	–
21/04/2010	18.7	19.6	−4.4	7.8	12.7	−38.5
21/07/2010	25.8	33.1	−22.1	21.1	–	–
16/09/2010	32.8	36.4	−9.9	25.8	28.3	−8.9
11/11/2010	37.8	39.8	−5.1	27.7	31.5	−12.1
19/01/2011	40.4	44.0	−8.3	–	35.3	–
04/04/2011	50.3	56.2	−10.6	–	43.8	–
07/09/2011	75.5	86.5	−12.7	–	68.3	–

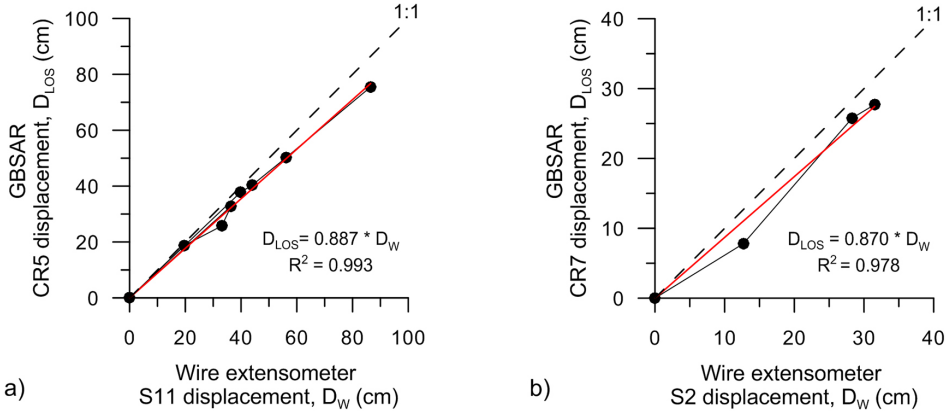

Fig. 8. Charts showing GB-SAR displacement against wire extensometer displacement: **(a)** for CR5 and S11, between February 2010 and September 2011, and **(b)** for CR7 and S2, between February 2010 and November 2010. The charts are created using the data included in Table 2. Red lines show the optimum linear fit to the data. Dashed lines show straight lines with a slope of 1 : 1.

The comparison of GB-SAR displacements and total displacements measured by extensometer (D_W) was done at three levels involving an increasing transformation of the data to account for systematic differences in displacements. The period compared was the whole of GB-SAR surveying, from February 2010 to September 2011.

A first comparison was carried out using the "raw" LOS displacements observed with GB-SAR (D_{LOS}) (Table 3 and Fig. 8). Despite the distance between the points observed with the two techniques, the two sets of data show good agreement (Fig. 8). In the two cases compared, D_{LOS} is proportional to D_W (Fig. 8 and Eq. 1). Therefore, the displacement measured by the two techniques shows a systematic difference which is proportional to D_W (Eq. 2). This difference is better expressed in Eq. (3) as a relative difference.

$$D_{LOS} = \alpha \cdot D_W \quad (1)$$

$$D_{LOS} - D_W = \alpha \cdot D_W - D_W = (\alpha - 1) \cdot D_W \quad (2)$$

$$\frac{D_{LOS} - D_W}{D_W} = (\alpha - 1), \quad (3)$$

where α is the slope of the regression lines at Fig. 8. Calculated as a percentage, the systematic relative difference in displacement between CR5 and S11 is −11.3 % and between CR7 and S2 is −13.0 %. After removing the systematic difference, the corresponding random errors are, on average, 0.4 cm and −0.6 cm. In the following the systematic differences are analysed.

The systematic difference between D_{LOS} and D_W is partially due to the fact that LOS displacement is a component of the total displacement. To account for this, a new comparison was carried out by using the total displacements (D_T) derived from the D_{LOS}. The transformation between D_{LOS} and D_T is described in Fig. 9. D_T is obtained as the magnitude of the projection of the vector $\boldsymbol{D}_{LOS}$ onto the unitary vector ($\boldsymbol{u}_T$) that defines the orientation of D_T. Therefore, D_T can be calculated by the equation

$$D_T = \frac{D_{LOS}}{\cos(\omega)}, \quad (4)$$

where ω is the angle between $\boldsymbol{D}_{LOS}$ and $\boldsymbol{u}_T$. For assessing ω, $\boldsymbol{u}_T$ must be previously determined from the 3-D components of the total displacement. The horizontal displacement

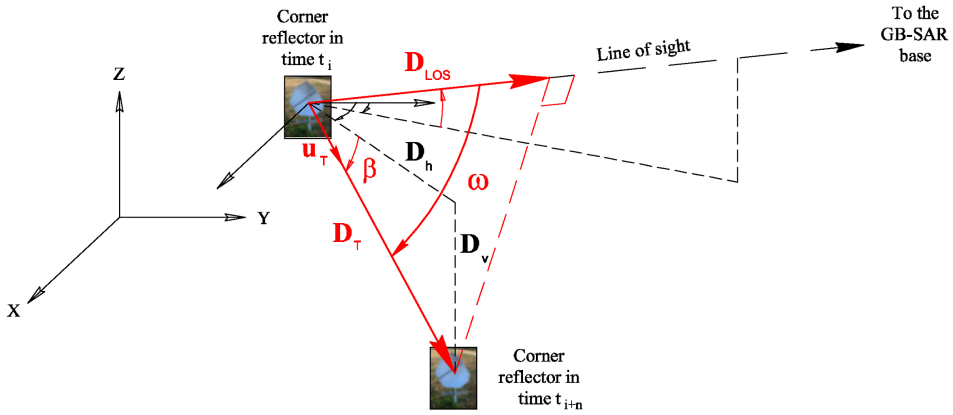

Fig. 9. Estimation of the total displacement (D_T) projecting the LOS displacement vector ($\boldsymbol{D}_{LOS}$) of the GB-SAR data onto the total displacement unitary vector ($\boldsymbol{u}_T$).

direction (azimuth) was calculated using the GPS monitoring data mentioned in Sect. 3.1. To minimize random error, the mean azimuth of the movement has been computed using the GPS data for the last seven years (2005 to 2012). Due to the lower accuracy of precise differential GPS for measuring vertical displacement, the vertical component β of $\boldsymbol{u}_T$ (Fig. 9) was obtained from the dip of the sliding surface, which is 10° on average.

The D_T calculated for CR5 and CR7 are shown in Table 4 and Fig. 10. In this case, we observe that D_T is again proportional to D_W in the two cases. Applying Eq. (3) using D_T instead D_{LOS}, we see that the systematic relative difference between D_T at CR5 and D_W at S11 is −4.5 %, and −0.2 % for CR7 and S2. After removing the systematic difference, the corresponding random errors are, on average, 0.4 cm and −0.7 cm.

The transformation of D_{LOS} to D_T reduced noticeably the relative difference in displacements between the CRs and the extensometers; however it is still significant for CR5 and S11. This difference is probably due to relative movement between the two points. In order to check this hypothesis, a comparison between the extensometers S11 and S9, which is 5 m away from CR5, have been computed. Due to S9 breaking before the onset of the GB-SAR, the correlation of the displacements recorded between December 1999 and August 2004 has been considered in the comparison. As it is shown in Fig. 11a, although the displacements observed at S9 are slightly lower than those at S11, they are linearly related. The obtained relationship allowed calculation of D_W at S9 for the period of GB-SAR surveying and then comparing it with the D_T determined for CR5 (Table 5 and Fig. 11b). Figure 11b shows that the total displacements at the two control points are very similar and that the slope of the plot is very close to 1 (0.6 % of systematic relative difference); this latter means that the systematic difference between CR5 and S11 is due to the relative displacements between both points.

4 Geomorphological interpretation of the displacement field

The GB-SAR-measured displacements together with the wire extensometry ones provide a more distributed view of the behaviour of the landslide (Fig. 12). In the following lines, the whole dataset (GB-SAR and wire extensometers) is used for interpreting the displacements field on terms of the landslide geomorphology.

The Vallcebre landslide, as previously mentioned, is formed by three main units. The lower unit is the most active and consequently the most extensively monitored. The presence of minor scarps in this unit indicates the existence of sub-units. At the north-western part of the unit a local translational slide (the so-called NW sub-unit), bounded by scarps up to 2 m high, was identified (Fig. 12). The toe of this local slide shows a lobate morphology which overrode the Vallcebre creek. In contrast, the rest of the toe of the lower landslide unit displays fresh and steep scarps resulting from the occurrence of small rotational failures induced by the erosion of the Vallcebre torrent.

Total displacements (D_T) estimated with GB-SAR between February 2010 and November 2010 (Table 4), which is the period with a maximum number of measured CRs (11 CRs), were used to analyse the relative movements within the lower landslide unit, together with the total displacements (Dw) observed in extensometers S2, S5, and S11. For CRs 1, 3, 4, 5, 7, and 8, the orientation of the displacement vector (D_T) was determined using precise differential GPS data, as was described in the previous section. CRs 2, 10, 11, 12, and 13 are located in the NW sub-unit where no GPS data are available. In these cases, D_T was determined using D_T azimuths calculated from the geomorphologic map, following directions parallel to the boundaries of the sub-unit. A map of the displacement field is shown in Fig. 12.

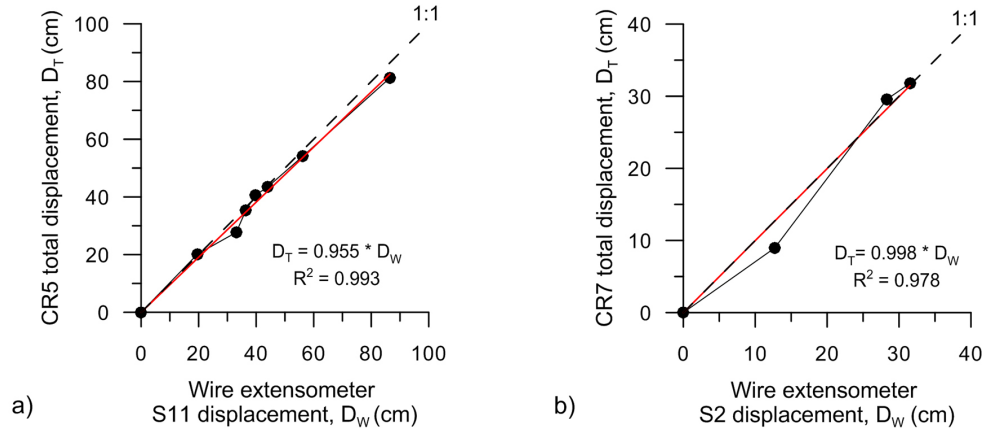

Fig. 10. Charts showing GB-SAR total displacement against wire extensometer displacement: **(a)** for CR5 and S11, between February 2010 and September 2011, and **(b)** for CR7 and S2, between February 2010 and November 2010. Red lines show the optimum linear fit to the data. Dashed lines show straight lines with a slope of 1 : 1.

Table 4. Total displacements in CRs (D_T) from February until November 2012 calculated from GB-SAR LOS displacements (D_{LOS}) using the angle between LOS and the total displacement vector.

CR	D_{LOS} [cm]		Close GPS target	Azimuth of displ. vector	w° (angle $D_{S,LOS}$, D_T)	$D_S/D_T(=\cos w)$	D_T [cm]	
	11/11/2010	07/09/2011					11/11/2010	07/09/2011
05	37.8	75.5	S8	295	21.6	0.93	40.6	81.2
07	27.7	–	S1	301	29.3	0.87	31.8	–
01	35.3	72.3	S8	295	22.9	0.92	38.3	78.5
03	33.5	76.7	R1	292	22.0	0.93	36.1	82.7
04	34.7	–	R1	292	22.1	0.93	37.4	–
08	35.6	–	S8	295	23.6	0.92	38.8	–
02	33.2	–	–	280	20.5	0.94	35.4	–
10	33.6	67.4	–	296	31.2	0.86	39.3	78.8
11	29.6	70.4	–	292	24.9	0.91	32.6	77.6
12	41.2	89.8	–	280	20.2	0.94	43.9	95.7
13	43.5	–	–	274	23.3	0.92	47.3	–

The average displacement of the lower unit for the mentioned period was 37.2 cm (corresponding to an average velocity of 1.3 mm day^{-1}), with a standard deviation of 7.1 cm. Most of the control points moved between 30 and 45 cm (12 of the 14 points), i.e. within 1σ. The two points that exhibited the largest relative displacement were CR13 (located at the toe of the unit, Fig. 11, with a displacement of 52 cm) and S5 (at the bottom of the head scarp of the unit, that moved only 21 cm); the differential displacement between them was 31 cm, i.e. four times the standard deviation (σ). This overall analysis indicates that the relative movements are significant within this landslide unit.

Relative movements in the lower landslide unit show a distinct behaviour. The minimum displacements are measured in the upper part, close to the head of the unit (at S5, S2, and CR7) (Fig. 12). The control points located at the toe of the unit (CR5, S11, CR3, and CR4) have displacements 37 % higher. In the frontal part of the toe (CR1 and CR8), the movement is 4 % slower, compared with points located in the same section (CR5 and S11), due to the change of dip of the sliding surface of the landslide along the slope direction in this zone. Here, the sliding surface has an upslope dip, a characteristic that is revealed by the counterslope tilting of the ground surface and the presence of ponds (Corominas et al., 2005). The upslope dip of the sliding surface involves an increase of the resistance to the landslide movement and, as a result, a decrease of the local displacement velocity. Despite this local reduction of velocity in the front, the overall behaviour is a downslope increase of the landslide velocity, as was mentioned above. This increase is interpreted as a consequence of the erosion of the landslide front by the torrent.

The existence of the NW sub-unit is also identified by the displacements measured with the GB-SAR. The average displacement of the NW sub-unit is 41 cm for the analysed period, whereas the rest of the landslide unit shows an average displacement of 35 cm (14 % lower) (Fig. 12). An increase of the rate of movement was also observed down the slope of the sub-unit, though it is not as well defined as in the rest

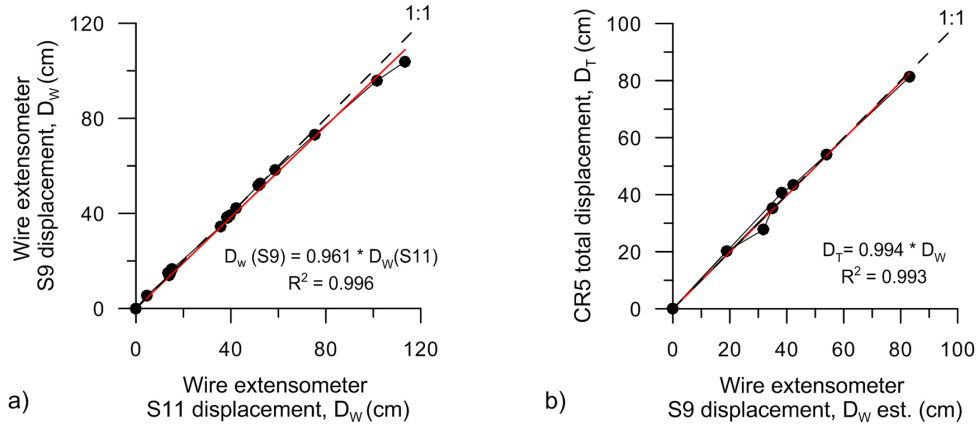

Fig. 11. (a) Chart comparing total displacement recorded at wire extensometers S11 and S9, from December 1999 to August 2004, and **(b)** chart comparing total displacement calculated for extensometer S9 and total displacement calculated for CR5 for the period from February 2010 to September 2010. Red lines show the optimum linear fit to the data. Dashed lines show straight lines with a slope of 1 : 1.

Table 5. Comparison of GB-SAR LOS displacements (D_{LOS}) measured for CR5 and CR7 and total displacements measured by wire extensometers (D_W) for S11 and S2, respectively.

Date	D_W S11 [cm]	D_W S9 [cm]	D_T CR5 [cm]	D_T CR5 estimated from D_W S9 [cm]	D_T CR5 – D_T CR5 estimated from S9 [cm]
09/02/2010	0	0.0	0.0	0.0	–
21/04/2010	19.6	18.8	20.2	18.7	1.5
21/07/2010	33.1	31.8	27.7	31.6	−3.9
16/09/2010	36.4	35.0	35.3	34.8	0.6
11/11/2010	39.8	38.2	40.6	38.0	2.6
19/01/2011	44	42.3	43.4	42.0	1.4
04/04/2011	56.2	54.0	54.1	53.7	0.4
07/09/2011	86.5	83.1	81.3	82.6	−1.3

of the unit. The highest displacements of the landslide front recorded at this sub-unit show an average of 46.4 cm (CR10 and CR13), in contrast to 38.7 cm shown by the front outside of this sub-unit (at CR1 and CR8). This higher velocity is consistent with the local lobate morphology of the toe of the sub-unit and with the fact that the toe is here overriding the Vallcebre torrent.

5 Conclusions

In this work, a new procedure based on GB-SAR data has been used to monitor the Vallcebre landslide located in the eastern Pyrenees. The procedure exploits the amplitude component of the GB-SAR images instead of using the classic interferometric approach. This fact has allowed overcoming some of the limitations of GB-SAR interferometry such as phase ambiguity and the atmospheric effects which act as critical constraints when monitoring slow landslides that demand non-continuous monitoring. It is worth noting that the need for using this approach on Vallcebre site was stimulated by the fact that by using exactly the same GB-SAR data described in this work, unsuccessful results were obtained by interferometry.

The results described in this paper use 13 CRs spread along the most active part of the landslide deployed during the period February 2010 to September 2011 that were used to carry out eight GB-SAR campaigns. The data obtained at five surveying campaigns based on the CRs pixels and data acquired by two extensometers located in the proximity of the CRs have been used to validate and compare the results. In addition, the use of GPS measurements allowed estimating the total displacements from GB-SAR LOS data and thus performing a more accurate comparison with wire extensometers. The experience of Vallcebre has shown the potentialities of the non-interferometric approach as centimetric precision and long-range monitoring. The most relevant results can be summarized in the following points: (i) the validation with the EDM measurements has confirmed the expected precision of 1 cm for those CRs with PBR higher than 30 dB, (ii) the GB-SAR measurements have evidenced

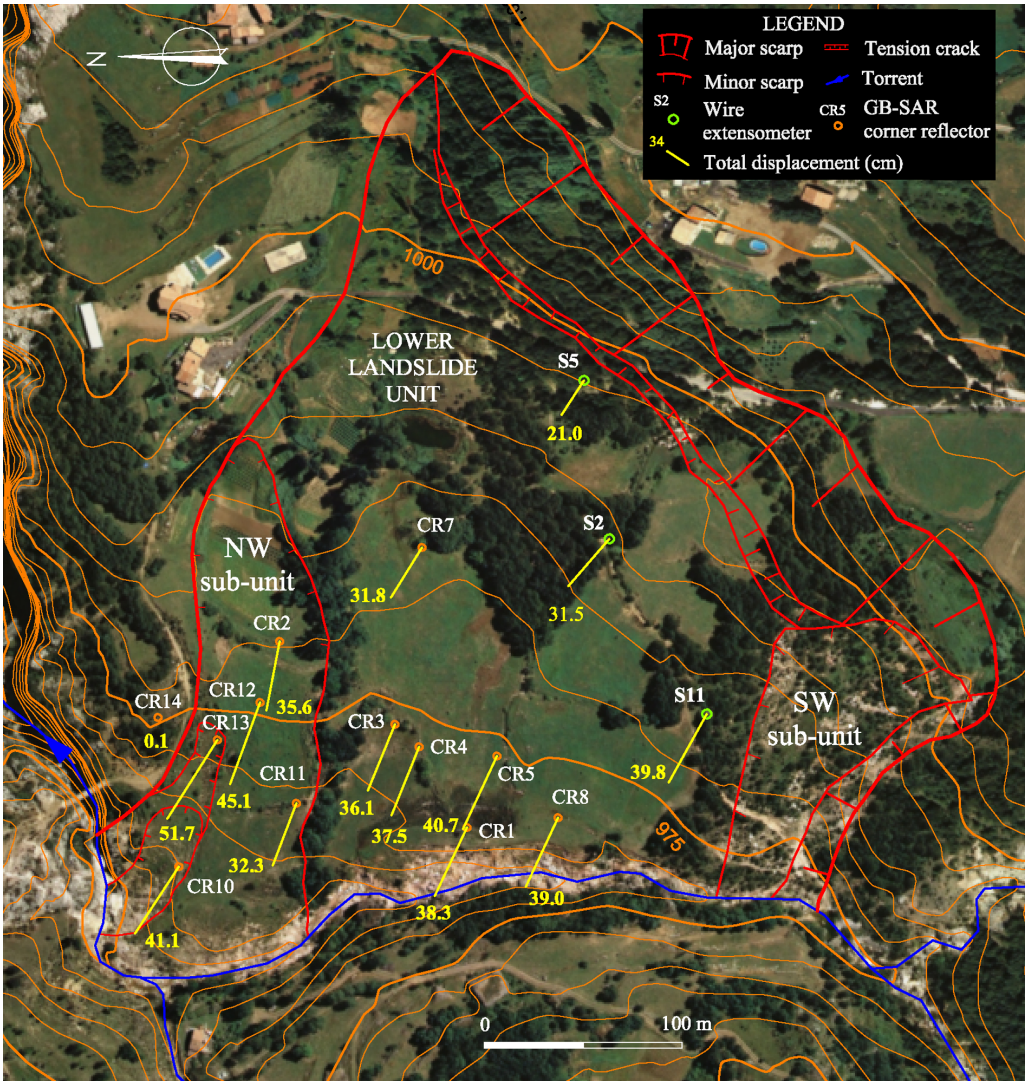

Fig. 12. Displacement field of the lower unit of the Vallcebre landslide reconstructed using GB-SAR CRs and borehole wire extensometers. Displacements are the total ones observed from 9 February 2010 to 11 November 2010. The CRs CR6, CR15, CR16, and CR17 are not included because they were installed after February 2010.

displacements of up to 80 cm between February 2010 and September 2011, and (iii) the results obtained with GB-SAR and extensometers showed good agreement. Despite the distance between the compared extensometers and the CRs, the relative differences between their measurements range from 4.5 % to 0.2 %; (iv) the geomorphologic analysis evidenced the consistency of the relative displacements measured within the moving area and the different sub-units of the landslide.

Viewed more generally, the presented results show the potentialities of the procedure for monitoring slow landslides, providing the ability to exploit the GB-SAR technique in an alternative way and opening a new range of applications. In addition, it is worth noting that from the point of view of measurements, the collected data can be processed using both interferometric and non-interferometric procedures. Compared with other geodetic techniques, although future developments are needed, it presents advantages which must be underlined:

– It can measure under any weather condition and at long distances (up to several km): this is a clear advantage with respect to all the existent optical techniques, which can reach comparable ranges only under perfect propagation conditions.

– Although the basic cost of the GB-SAR system can be relatively high, the cost of the survey is low compared with in-hole techniques.

– Compared with optical and interferometric techniques it can be easily extended to total automatic procedures because it did not ask for depth skill on data interpretation during the data acquisition.

Moreover, the technique demands more research efforts in order to improve some aspects which limit its operational aspects. To date, the main constraint of the technique is the need for deploying artificial CRs, which limits severely the remote sensing application. However, it must be underlined that the CRs have been used to obtain the best performances in terms of accuracy. Further work will be devoted to exploiting the same approach using natural reflectors, thus reducing the need for artificial reflectors. For this purpose, different matching algorithms will be investigated. Another important aspect to be addressed is the design of advanced, simple and easy to install reflectors. The use of active reflectors (transponders) could drastically reduce the size and improve the logistics of the procedure. Last, but not least, more efforts must be devoted to exploiting the potentiality of the proposed procedure to provide accurate cross-range measurements, which at the moment does not offer the best performance in terms of accuracy.

Acknowledgements. This work has been partially funded by the FP7 project Safeland (http://www.safeland-fp7.eu) and the project SAXA funded by AGAUR (Government of Catalonia). The corner reflectors used have been developed within the framework of collaboration between the Institute of Geomatics and the Fundación Ciudad de la Energia (http://www.ciuden.es). To conclude, the authors want to thank Adrià Perez for his collaboration in some campaigns and his participation in the surveying data analysis.

Edited by: V. Tofani
Reviewed by: three anonymous referees

References

Alba, M., Bernardini, G., Giussani, A., Ricci, P. P., Roncoronia, F., Scaioni, M., Valgoic, P., and Zhangd, K.: Measurement of dam deformations by terrestrial interferometric techniques, International Archives of the Photogrammetry, Remote Sensing and Spatial Information Sciences, 37, Part B1, Beijing (China), 2008.

Antonello, G., Casagli, N., Farina, P., Fortuny, J., Leva, D., Nico, G., Sieber, A. J., and Tarchi, D.: A ground-based interferometer for the safety monitoring of landslides and structural deformations, Proc. of International Geoscience and Remote Sensing Symposium, (IGARSS), 1, 218–220, Seoul (South Korea), 2003.

Antonello, G., Casagli, N., Farina, P., Leva, D., Nico, G., Sieber, A. J., and Tarchi, D.: Ground-based SAR interferometry for monitoring mass movements, Landslides, 1, 21–28, 2004.

Casagli, N., Tibaldi, A., Merri, A., Del Ventisette, C., Apuani, C., Guerri, L., Fortuny-Guasch, J., and Tarchi, D.: Deformation of Stromboli Volcano (Italy) during the 2007 eruption re-vealed by radar interferometry: Numerical modelling and structural geological field data, J. Volcanol. Geotherm. Res., 182, 182–200, 2009.

Casagli, N., Catani, F., Del Ventisette, C., and Luzi, G.: Monitoring, prediction, and early warning using ground-based radar interferometry, Landslides, 7, 291–301, 2010.

Corominas, J., Moya, J., Lloret, A., Gili, J. A., Angeli, M. G., Pasuto A., and Silvano, S.: Measurement of landslide displacements using a wire extensometer, Eng. Geol., 55, 149–166, 2000.

Corominas, J., Moya, J., Ledesma, A., Lloret, A., and Gili, J.: A Prediction of ground displacements and velocities from groundwater level changes at the Vallcebre landslide (Eastern Pyrenees, Spain), Landslides, 2, 83–96, 2005.

Crosetto, M., Monserrat, O., Luzi, G., Cuevas-Gonzalez, M., and Devanthery, N.: A Noninterferometric Procedure for Deformation Measurement Using GB-SAR Imagery, IEEE Geosci. Remote S., 99, 1 pp., 2013a.

Crosetto, M., Gili, J. A., Monserrat, O., Cuevas-González, M., Corominas, J., and Serral, D.: Interferometric SAR monitoring of the Vallcebre landslide (Spain) using corner reflectors, Nat. Hazards Earth Syst. Sci., 13, 923–933, doi:10.5194/nhess-13-923-2013, 2013b.

Cruden, D. M. and Varnes, D. J.: Landslide types and processes. Landslides-Investigation and Mitigation, Special Report, 247, 36–75, 1996.

Del Ventisette, C., Intrieri, E., Luzi, G., Casagli, N., Fanti, R., and Leva, D.: Using ground based radar interferometry during emergency: the case of the A3 motorway (Calabria Region, Italy) threatened by a landslide, Nat. Hazards Earth Syst. Sci., 11, 2483–2495, doi:10.5194/nhess-11-2483-2011, 2011.

Fortuny-Guasch, J.: A Fast and Accurate Far-Field Pseudopolar Format Radar Imaging Algorithm", IEEE T. Geosci. Remote Sens., 47, 1187–1196, April 2009.

Gili, J. A., Corominas, J., and Rius, J.: Using Global Positioning System techniques in landslide monitoring, Eng. Geol., 55, 167–192, 2000.

Gili, J. A., Corominas, J., and Moya, J.: Wire extensometers, in: Evaluation report on innovative monitoring and remote sensing methods and future technology, edited by: Tofani, V., Segoni, S., Catani, F., and Nicola Casagli, N., Deliverable 4.5 of the European Project SAFELAND, 12–16, available at: http://www.safeland-fp7.eu., 2012.

Herrera, G., Fernandez-Merodo, J. A., Mulas, J., Pastor, M., Luzi, G., and Monserrat, O.: A landslide forecasting model using ground based SAR data: the Portalet case study, Eng. Geol., 105, 220–230, 2009.

Leva, D., Nico, G., Tarchi, D., Fortuny, J., and Sieber, A. J.: Temporal analysis of a landslide by means of a ground-based SAR interferometer, IEEE Trans. Geosci. Remote Sens., 41, 745–752, 2003.

Luzi, G.: Ground-based SAR Interferometry: a novel tool for Geoscience, Geosci. Remote Sens., New Achievements, 01-026, edited by: Imperatore, P. and Riccio, D., Vukopvar, Croatia, 2010.

Luzi, G., Pieraccini, M., Mecatti, D., Noferini, L., Macaluso, G., Tamburini, A., and Atzeni, C.: Monitoring of an Alpine Glacier by Means of Ground-Based SAR Interferometry, IEEE. Geosci. Remote Sens. Lett., 4, 495–499, 2007.

Monserrat, O.: Deformation measurement and monitoring with Ground-Based SAR, Ph.D. thesis, Universitat Politècnica de Catalunya, 2012.

Noferini, L., Pieraccini, M., Mecatti, D., Luzi, G., Tamburini, A., Broccolato, M., and Atzeni, C.: Permanent scatterers analysis for atmospheric correction in ground-based SAR interferometry, IEEE T. Geosci. Remote Sens., 43, 7, 1459–1471, 2005.

Pieraccini, M., Casagli, N., Luzi, G., Tarchi, D., Mecatti, D., Noferini, L., and Atzeni, C.: Landslide Monitoring by Ground-Based Radar Interferometry: a field test in Valdarno (Italy), Int. J. Remote Sens., 24, 1385–1391, 2002.

Rödelsperger, S., Läufer, G., Gerstenecker, C., and Matthias, B.: Monitoring of displacements with ground-based microwave interferometry, IBIS-S and IBIS-L, J. Appl. Geodesy, 4, 41–54, 2010.

Strozzi, T., Werner, C., Wiesmann, A., and Wegmüller, U.: Topography mapping with a portable real aperture radar interferometer, Geosci. Remote Sens. Lett., 9, 277–281, doi:10.1109/LGRS.2011.2166751, 2011.

Tarchi, D., Rudolf, H., Luzi, G., Chiarantini, L., Coppo, P., and Sieber, A. J.: SAR interferometry for structural changes detection: A demonstration test on a dam, in: Proc. International Geosci. Remote Sens. Symposium, IGARSS, 1522–1524, Hamburg Germany, 1999.

Tarchi, D., Casagli, N., Fanti, R., Leva, D., Luzi, G., Pasuto, A., Pieraccini, M., and Silvano, S.: Landslide monitoring by using ground-based SAR interferometry: an example of application, Eng. Geol., 68, 1–2, 15–30., 2003.